Molecular Crystals and Liquid Crystals

Publication details, including instructions for authors and subscription information:
http://www.tandfonline.com/loi/gmcl20

Thermal Properties and Photo-Polymerization of Diepoxy Monomers with Mesogenic Group

N. Tokushige [a] , T. Mihara [a] & N. Koide [a]

[a] Department of Chemistry, Faculty of Science, Science University of Tokyo, Tokyo, Japan

Version of record first published: 31 Aug 2006

To cite this article: N. Tokushige, T. Mihara & N. Koide (2005): Thermal Properties and Photo-Polymerization of Diepoxy Monomers with Mesogenic Group, Molecular Crystals and Liquid Crystals, 428:1, 33-47

To link to this article: http://dx.doi.org/10.1080/154214090892681

Mol. Cryst. Liq. Cryst., Vol. 428, pp. 33–47, 2005

ISSN: 1542-1406 print/1563-5287 online
DOI: 10.1080/154214090892681

Taylor & Francis
Taylor & Francis Group

Thermal Properties and Photo-Polymerization of Diepoxy Monomers with Mesogenic Group

N. Tokushige
T. Mihara
N. Koide
Department of Chemistry, Faculty of Science, Science University of Tokyo, Tokyo, Japan

We synthesized two diepoxy monomers containing a mesogenic group to investigate thermal conductivity of the resulting epoxy resins prepared by photo-polymerization of the monomers. One diepoxy monomer shows an enantiotropic nematic phase, whereas the other displayed enantiotropic smectic A and nematic phases. The epoxy resins were prepared by cationic photo-polymerization of the diepoxy monomers in the liquid-crystalline (LC) state. The structures of LC phases for each diepoxy monomer were fixed in the thin films of epoxy resins. Thermal conductivity of the LC epoxy resins was larger than that of the conventional epoxy resins. The epoxy resin prepared by photo-polymerization of the monomer in the smectic A phase displayed larger thermal conductivity than that in the nematic phase.

Keywords: epoxy resin; liquid-crystalline polymer; thermal conductivity; thermoset

INTRODUCTION

In recent years, downsizing and high performance of electronic apparatuses cause an increasing quantity of heat generated by the internal conductors. One approach to diffuse the heat is the use of the composites of thermosets with metals or ceramics because of the low thermal conductivity of thermosets themselves. However, the composite materials applied to the thermal conductive material have a lots of disadvantages such as limitation of amounts of the fillers, poor processability and so forth. Therefore, it is necessary to design new thermosets that have a capability of releasing the heat generated in the electric apparatuses

Address correspondence to N. Koide, Department of Chemistry, Faculty of Science, Science University of Tokyo, 1-3 Kagurazaka, Shinjuku-ku, Tokyo 162-8601, Japan. Tel.: +81-3-5228-8248, Fax: +81-3-3235-2214, E-mail: nkoide@ch.kagu.sut.ac.jp

smoothly. Thermal conductivity of the insulator-like thermosets depends deeply on the conduction of phonon. It is necessary to control the diffraction of the phonon to improve the thermal conductivity of the thermosets. One candidate to control the diffraction of the phonon would be formed by the nanolevel high-order structure introduced by the self-organizing structure into the conventional resins.

Ordered polymeric structures can be easily obtained by self-organizing systems such as liquid-crystal polymers (LCPs). LC phases are generally observed as intermediates between solid and isotropic liquid fluid. The LC phase of the LCP is sustained upon cooling through glass-transition temperature to room temperature. In some cases, the orientation of mesomorphic state of the LCPs can be locked in by the photo-reaction and/or crosslinking reagent. Such anisotropic LCP networks have the possibility of application for electro-optic materials [1,2]. Several methods have been known to obtain anisotropic LCP networks. Anisotropic LCP networks can be produced by in situ polymerization of reactive molecules in the LC state. Polymerization is photochemically induced after the induction of long-range orientation of the molecules in a desired LC phase. Lightly crosslinked LCPs have elastomeric properties and can be easily stretched to obtain oriented systems [3]. The in situ photo-polymerization of the oriented LC monomers also provided the highly oriented LCP networks (LC thermosets). Bifunctional LC acrylate monomers were often used with monofunctional LC acylate monomer and/or nonreactive LC for the preparation of the LC thermosets [4–6].

Another attempt to obtain the LC thermosets has been performed by a curing reaction of LC diepoxy compounds with amine compounds. Many researchers have investigated synthesis and thermal behavior of LC epoxy resins for the preparation of the films with anisotropic optical properties [7–13]. Stilbene, benzoate, and biphenyl groups were employed for the mesogenic core of LC diepoxy monomers, whereas aromatic diamine derivatives were often used for the curing agent.

Amorphous epoxy resins are widely used in sealant for electronic devices, because of their good mechanical, electrical, and thermal properties and reasonable economic price. So, by a combination of the amorphous epoxy resin and mesogenic core, the polymers obtained would demonstrate a highly ordered crystal-like structure. Takezawa et al. had reported that LC epoxy resins with biphenyl or phenylbenzoate groups displayed higher thermal conductivity [14–16]. The LC epoxy resins were prepared by curing reactions of the LC diepoxy compound with the aromatic diamine compound. The value of the thermal conductivity for the LC epoxy resins was about five times as large as that for the conventional epoxy resins.

In this study, we synthesized two kinds of diepoxy mesogenic monomers to obtain the LC epoxy resins by cationic photo-polymerization [17,18] and examined the thermal properties of the LC epoxy resins. We expect that the LC state of an epoxy LC monomer would be easily fixed by photo-polymerization in the LC state.

EXPERIMENTAL

Materials

Diepoxy mesogenic monomers 1 and 2 were prepared according to the conventional synthetic method as shown in Schemes 1 and 2, respectively. The diepoxy mesogenic monomer as shown in Scheme 1 was synthesized according to the literature [7]. Synthetic procedures of the diepoxy monomers are described below.

10-Undecenyl-4-Toluenesulfonate (1)

10-Undecen-1-ol (42.5 g, 0.245 mol) was dissolved in pyridine (100 ml) under nitrogen atmosphere. p-Toluenesulfonyl chloride

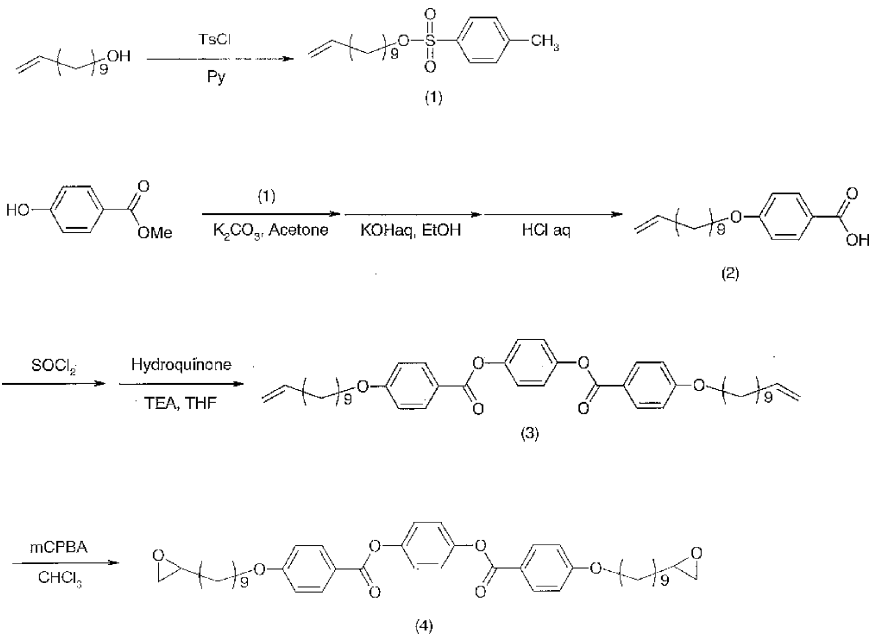

SCHEME 1 Synthesis of diepoxy monomer 1.

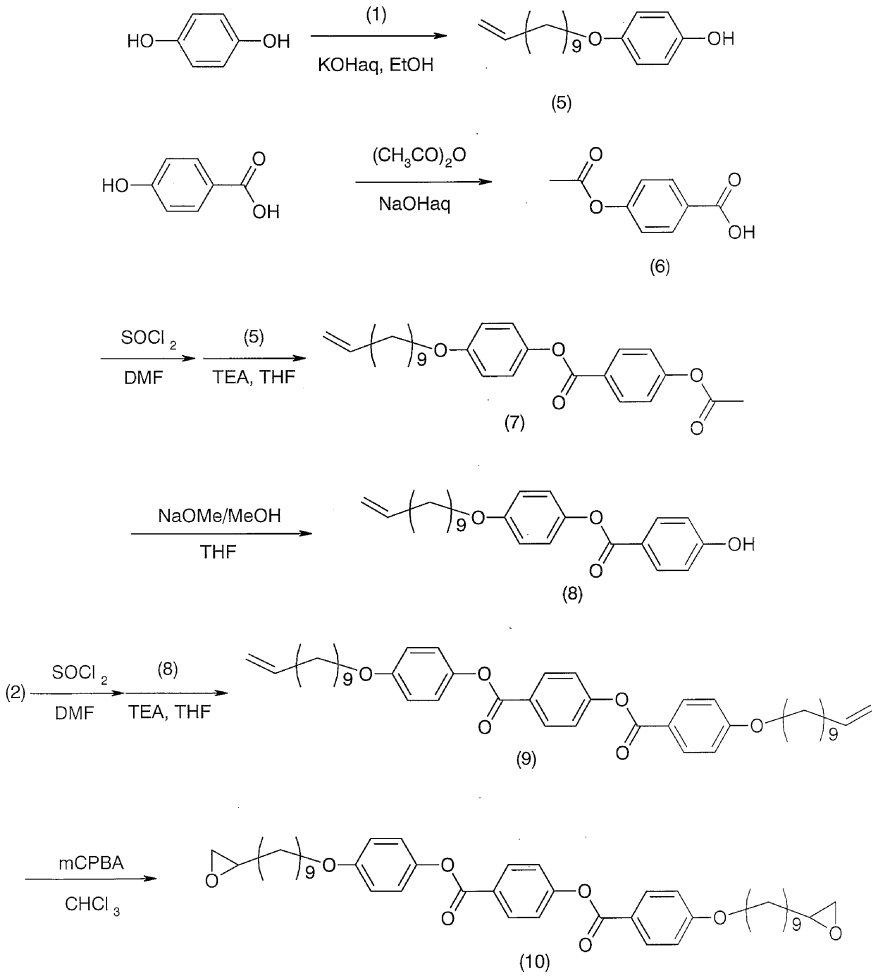

SCHEME 2 Synthesis of diepoxy monomer 2.

(52.4 g, 0.278 mol) was added to the pyridine solution in an ice bath. After the reaction mixture was stirred for 12 h, a large quantity of water was added to the reaction mixture in an ice bath. In addition, the mixture was stirred for 6 h at room temperature. The product was extracted with a large quantity of chloroform. After the chloroform solution was dried under magnesium sulfate, chloroform was evaporated to dryness under reduced pressure. The colorless liquid was obtained in an 84% yield (74.2 g). The product was used without further purification.

^{1}H-NMR (nuclear magnetic resonance) ($CDCl_3$) δ ppm: 7.8 (2H, d, Ar), 7.3 (2H, d, Ar), 5.8 (1H, m, allyl), 4.9–5.0 (2H, m, allyl), 4.0 (2H, t, CH_2O), 2.4 (3H, s, Ar–CH_3), 2.0 (2H, t, CH_2), 1,7 (2H, t, CH_2), 1.2–1.4 (12H, m, CH_2). IR (neat) ν cm^{-1}: 1641 (C=C, allyl), 1598, 1495 (Ar), 1363, 1178 (O=S=O), 954, 912, 815 (S–O–C).

4-(10-Undecenyloxy)Benzoic Acid (2)

Methyl-4-hydroxybenzoate (10.0 g, 65.7 mmol) was dissolved in acetone (250 ml). Potassium carbonate (27.2 g, 0.197 mol) was added to the acetone solution. After that, the compound (1) (25.2 g, 77.7 mol) was added dropwise to the acetone solution. The reaction mixture was refluxed for 12 h. The filtrate was evaporated to dryness and the residue was dissolved in ethanol (100 ml). Aqueous potassium hydroxide was added to the ethanol solution and the mixture was refluxed for 30 min. After the ethanol was evaporated, aqueous HCl was added to the residue and then the mixture was refluxed for 3 h. The solid obtained was washed with water and ethanol. The product was obtained in a 72% yield (19.1 g).

^{1}H-NMR (DMSO) δ ppm: 7.8 (2H, d, Ar), 7.0 (2H, d, Ar), 5.8 (1H, m, allyl), 4.9–5.0 (2H, m, allyl), 4.0 (2H, t, CH_2O), 2.0 (2H, t, CH_2), 1,7 (2H, t, CH_2), 1.3–1.4 (12H, m, CH_2). IR (neat) ν cm^{-1}: 3300–2500 (OH, carboxylic acid group), 1670 (C=O, carboxylic acid group), 1606 (Ar).

4-(10-Undecenyloxy)Benzoic Acid 1,4-Phenylene Ester (3)

Thionyl chloride (20 ml) and a small amount of N,N-dimethyl formamide were added to the compound (2) (8.4 g, 28.9 mmol). The mixture was stirred at 70°C for 4 h. After excess thionyl chloride was removed under reduced pressure, the residue was dissolved in dry tetrahydrofuran (THF). The THF solution was added dropwise to the THF solution (100 ml) of hydroquinone (1.44 g, 13.0 mmol) and triethylamine (1.6 ml) in an ice bath. The reaction mixture was stirred at room temperature for 9 h. After THF was evaporated under reduced pressure, the residue was washed with water and methanol. The product was purified by silica-gel column chromatography (eluent: chloroform). The product was obtained in an 80% yield (7.6 g).

^{1}H-NMR ($CDCl_3$) δ ppm: 8.1 (4H, d, Ar), 7.2 (4H, d, Ar), 6.9 (4H, d, Ar), 5.7 (2H, m, allyl), 4.8–4.9 (4H, m, allyl), 4.0 (4H, t, CH_2O), 2.0 (4H, t, CH_2), 1.7 (4H, t, CH_2), 1.2–1.4 (24H, m, CH_2). IR (nujol) ν cm^{-1}: 1725 (C=O, ester group), 1641 (C=C, allyl), 1608, 1513 (Ar).

4-(9-Oxiranylnonanoxy)Benzoic Acid 1,4-Phenylene Ester (4)

The chloroform solution of 65% m-chloroperbenzoic acid (mCPBA) (3.48 g, 13.3 mmol) was added dropwise to the chloroform solution

(100 ml) of compound (3) (3.64 g, 5.54 mmol). The reaction mixture was refluxed for 24 h. The filtrate was washed with 5% aqueous sodium sulfite, 5% aqueous sodium hydrogen carbonate, and 30% aqueous sodium chloride, and then the chloroform solution was dried under magnesium sulfate. After chloroform was removed under reduced pressure, the residue was washed with methanol. The product was purified by silica-gel column chromatography (eluent: chloroform). The product was obtained in a 47% yield (1.87 g).

^{1}H-NMR ($CDCl_3$) δ ppm: 8.1 (4H, d, Ar), 7.2 (4H, d, Ar), 4.1 (4, t, CH_2O), 2.8 (2H, s, CH epoxy), 2.7 (2H, m, CH epoxy), 2.4 (2H, m, CH epoxy), 1.8 (4H, m, CH_2), 1.3–1.8 (28H, m, CH_2). IR (nujol) ν cm^{-1}: 1727 (C=O, ester group), 1604, 1511 (Ar), 912 (C−C, epoxy ring).

4-(10-Undecenyloxy)Phenol (5)

Aqueous potassium hydroxide (13.4 g, 0.238 mmol) (100 ml) was added to the ethanol solution of hydroquinone (30.6 g, 0.278 mmol) and a small amount of tetra-n-butylammonium bromide. After the compound (1) (23.1 g, 79.5 mmol) was added dropwise to the ethanol solution, the reaction mixture was refluxed for 24 h. Ethanol was removed under reduced pressure. The residue was extracted with chloroform. The chloroform solution was dried over magnesium sulfate. Chloroform was evaporated under reduced pressure and then the residue was dissolved in methanol. Methanol was evaporated under reduced pressure. The product was used without further purification. The product was a 56% yield (11.6 g).

^{1}H-NMR ($CDCl_3$) δ ppm: 6.8 (4H, q, Ar), 5.8 (1H, m, allyl), 4.9–5.0 (2H, m, allyl), 4,7 (1H, s, Ar−OH), 3.9 (2H, t, CH_2O), 2.1 (2H, t, CH_2), 1.7 (2H, t, CH_2), 1.3–1.4 (12H, m, CH_2).

4-(10-Undecenyloxy)Phenyl-4-[(10-Undecenyloxy) Benzyloxy]Benzoate (9)

Thionyl chloride and a small amount of N,N-dimethyl formamide were added to p-acetoxybenzoic acid (6) (5.72 g, 41.3 mmol), and then the mixture was stirred at 70°C for 4 h. After excess thionyl chloride was removed under reduced pressure, the tetrahydrofuran (THF) solution (50 ml) of the residue was added dropwise to the THF solution (l00 ml) of the compound (5) (8.33 g, 31.7 mmol) and triethylamine (9.6 ml) on ice bath under nitrogen atmosphere. The reaction mixture was stirred for 9 h at room temperature. After THF was evaporated to dryness, the residue was washed with water and methanol. The crude product (7) was obtained in an 81% yield (10.6 g).

Twenty-eight percent methanol solution of sodium methoxide (4.34 g, 22.3 mmol) was added to the THF solution (50 ml) of the crude

product (7) (9.5 g, 22.3 mmol). After the reaction mixture was stirred for 10 min, the reaction mixture was poured into aqueous HCl. The precipitate (8) was obtained in an 86% yield (7.33 g).

The compound (2) (5.0 g, 17.2 mmol) was dissolved in thionyl chloride (20 ml) containing a small amount of N,N-dimethyl formamide. After the mixture was stirred at 4 h at 70°C, excess thionyl chloride was removed under reduced pressure. The THF solution (50 ml) of the residue was added dropwise to the THF solution (l00 ml) of the compound (8) (6.67 g, 17.4 mmol) and triethylamine (5 ml) in an ice bath under nitrogen atmosphere. The reaction mixture was stirred for 9 h at room temperature. THF was evaporated under reduced pressure. The crude product was washed with water and methanol. The product was purified by silica-gel column chromatography (eluent: chloroform). The product was obtained in an 82% yield (9.2 g).

^{1}H-NMR ($CDCl_3$) δ ppm: 8.2 (2H, d, Ar), 8.1 (4H, d, Ar), 7.3 (2H, d, Ar), 7.1 (2H, d, Ar), 6.9 (2H, d, Ar), 6.8 (2H, d, Ar), 5.8 (2H, m, allyl), 4.8–4.9 (4H, m, allyl), 4.0 (2H, t, CH_2O), 3.9 (4H, t, CH_2O), 2.0 (4H, t, CH_2), 1.7 (4H, m, CH_2), 1.2–1.4 (24H, m, CH_2). IR (nujol) ν cm^{-1}: 1743, 1733 (C=O, ester group), 1643 (C=C, allyl), 1606, 1513 (Ar).

4-(10,11-Epoxyundecenyloxy)Phenyl-4-[(10,11-Epoxyundecenyloxy)Benzyloxy]Benzoate (10)

After 65% chloroform solution of m-chloro perbenzoic acid (mCPBA) (6.46 g, 24.3 mmol) was added dropwise to the chloroform solution (100 ml) of the compound (9) (6.67 g, 10.3 mmol), the reaction mixture was refluxed for 24 h. The filtrate was washed with 5% aqueous sodium sulfite, 5% aqueous sodium hydrogen carbonate, and 30% aqueous sodium chloride. The chloroform solution was dried over magnesium sulfate. Chloroform was evaporated to dryness and then the residue was washed with methanol. The product was purified by silica-gel column chromatography (eluent: chloroform). The product was obtained in a 48% yield (3.4 g).

^{1}H-NMR ($CDCl_3$) δ ppm: 8.3 (2H, d, Ar), 8.2 (2H, d, Ar), 7.4 (2H, d, Ar), 7.2 (2H, d, Ar), 7.1 (2H, d, Ar), 6.9 (2H, d, Ar), 4.1 (2H, t, CH_2O), 3.9 (2H, t, CH_2O), 2.9 (2H, d, CH epoxy), 2.8 (2H, m, CH epoxy), 2.5 (2H, m, CH epoxy), 1.8 (4H, m, CH_2), 1.3–1.6 (28H, m, CH_2). IR (nujol) ν cm^{-1}: 1743, 1733 (C=O, ester group), 1606, 1513 (Ar), 910 (C–C, epoxy ring).

Photo-Polymerization of Mesogenic Diepoxy Monomers

Diepoxy monomer (98 wt%), diphenyliodonium hexafluoroarsenate (1 wt%), 2,2′-dimethoxy-2-phenylacetophenone (0.5 wt%) and

isopropyl-9H-thioxantene-9-one (0.5 wt%) were dissolved in dichloromethane (30 ml). After evaporation of the solvent, the resulting mixture was dried in vacuum. The mixture in the glass cell (10 μm) was irradiated with a 500 W super high-pressure mercury lamp ($\lambda_{max} = 365$ nm, 2 mW cm^{-2} at 365 nm) in the mesophase (at 140°C and 120°C for monomers 1 and 2, respectively) for 10 min.

The films (thickness of about 1 mm) of epoxy resins were also prepared for thermal conductivity measurements in the same manner as above photo-polymerization condition.

Characterization

^{1}H-NMR measurements were carried out with a JEOL JNM-LA 400 spectrometer. Infrared spectra were recorded on a JEOL JIR 7000 spectrometer. Spectra were collected at 4 cm^{-1} resolution. Differential scanning calorimetry (DSC) measurements were conducted with a Mettler DSC821^e. Isothermal UV-DSC measurements were carried out with a Mettler DSC822^e equipped with a HAMAMATSU PHOTOCURE 200 UV-spot light source. Thermogravimetric analysis (TGA) was carried out using a Mettler TG50 system in air. Optical microscopy measurements were performed on a Nikon polarizing optical microscope, OPTIPHOTO-POL, equipped with a Mettler FP80 controller and a FP82 hot stage. X-ray diffraction patterns were recorded with a RIGAKU RINT2500 with Ni-filtered Cu-Kα radiation. The sample in quartz capillary (diameter 1 mm) and epoxy resin film were held in a temperature-controlled cell (RIGAKU LC high temperature controller). Thermal conductivity of epoxy resins was calculated from thermal diffusivity (laser flush method, RIGAKU LF/TCM-FA8510B), density, and heat capacity. The film of 10 mm in diameter and 1 mm in thickness was prepared for the laser flush method by cutting the epoxy resins.

RESULTS AND DISCUSSION

The chemical structures of the diepoxy mesogenic monomers (DMs) are shown in Fig. 1. Synthesis of two DMs is described in Schemes 1 and 2, respectively. We use the benzoate-type mesogenic cores with different ester sequences. One is a mesogenic core with a hydroquinone moiety in the center of the mesogenic core; the other is a mesogenic core with a hydroxy benzoic acid moiety.

Phase transition temperatures of DMs are summarized in Table 1. A schlieren texture was observed on both heating and cooling runs for DM1. Two peaks were detected in the DSC curves of DM1 on both

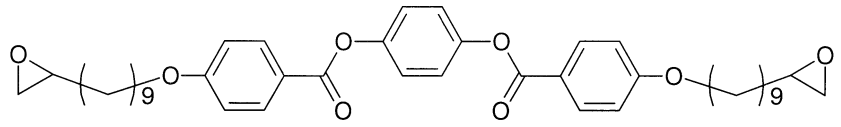

Diepoxy mesogenic monomer 1 (DM1)

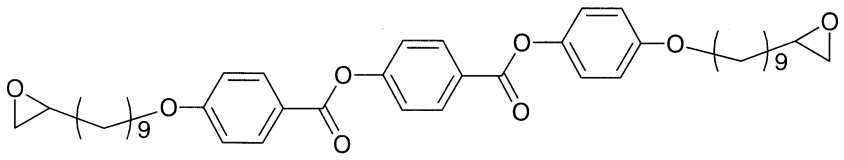

Diepoxy mesogenic monomer 2 (DM2)

FIGURE 1 Chemical structures of diepoxy monomers.

heating and cooling runs. The two peaks were assigned to melting and clearing points, respectively.

A small peak in the small-angle region (d-spacing; 40.1 Å) and a board peak in the wide-angle region were observed in the X-ray diffraction pattern of DM1 in the mesomorphic temperature range. The structure of the mesophase for DM1 would be a cybotactic nematic phase, because the peak in the small-angle region would be too small to be assigned to the diffraction peak because of the smectic layer structure.

Four peaks were detected in the DSC curves of DM2 on both heating and cooling runs. The four peaks would be assigned to phase-transition temperature of crystal–crystal, crystal–mesophase, mesophase–mesophase, and mesophase–isotropic fluid, respectively, based upon optical microscopic observation and X-ray diffraction measurements. The homeotropic alignment of DM2 in the lower

TABLE 1 Phase-Transition Temperatures of Diepoxy Monomers

Diepoxy monomers	Phase transition temperatures, °C
DM1	$\mathrm{Cr} \underset{99}{\overset{110}{\rightleftharpoons}} \mathrm{N} \underset{165}{\overset{165}{\rightleftharpoons}} \mathrm{I}$
DM2	$\mathrm{Cr} \underset{62}{\overset{86}{\rightleftharpoons}} \mathrm{Cr'} \underset{78}{\overset{87}{\rightleftharpoons}} \mathrm{SmA} \underset{143}{\overset{143}{\rightleftharpoons}} \mathrm{N} \underset{162}{\overset{162}{\rightleftharpoons}} \mathrm{I}$

Cr, Cr′: crystal; SmA: smectic A; N: nematic; I: isotropic phase.

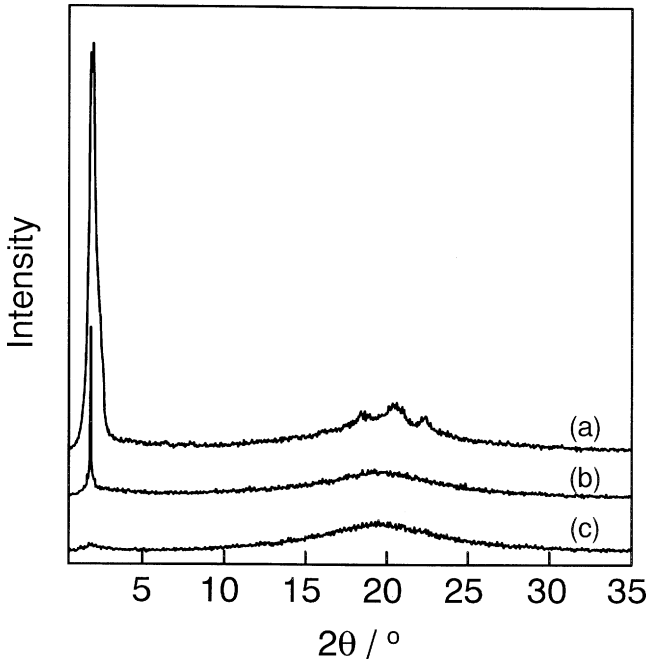

FIGURE 2 X-ray patterns of diepoxy monomer 2 at 86°C (a), 120°C (b), and 150°C (c) on heating run.

mesomorphic temperature range was confirmed by conoscopic observation of optical microscopy measurements, whereas a schlieren texture was observed in the higher mesomorphic temperature range of DM2. Figure 2 displays the X-ray diffraction patterns of DM2. The phase structure of DM2 at 86°C would be a crystal, because plural peaks are detected in the wide-angle region of the X-ray diffraction pattern.

A sharp peak in the small-angle region and a broad peak in the wide-angle region are observed in the X-ray diffraction pattern of DM2 at 120°C. The structure of the mesophase for DM2 at 120°C would be a smectic phase. The d-spacing resulting from the peak in the small-angle region is 48 Å, whereas the calculated length of DM2 with all-trans conformation is 41 Å. The structure of the mesophase for DM2 in the lower mesomorphic temperature range would be a smectic A_1 phase, although the d-spacing resulting from the peak in the small-angle region is slightly longer than that of the calculated length of DM2. In the higher mesomorphic temperature range (at 150°C), a sharp peak in the small-angle region disappears and a

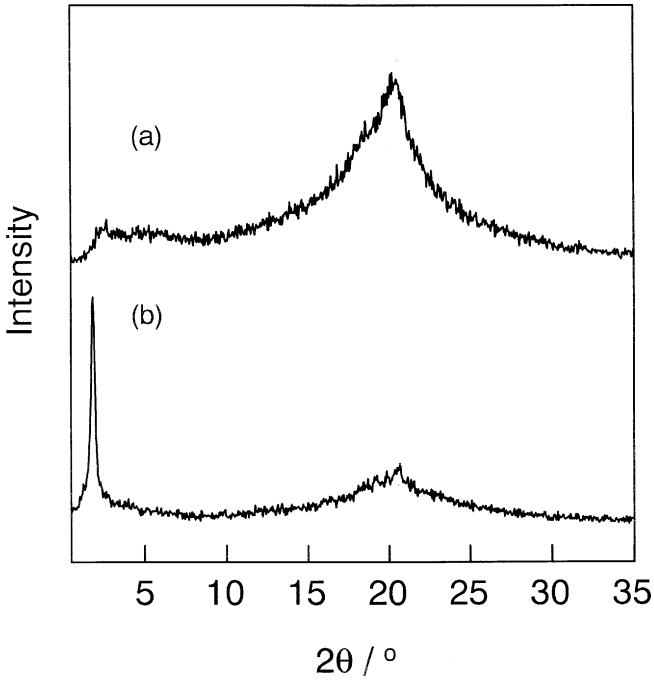

FIGURE 3 X-ray pattern of epoxy resin 1 (a) and 2 (b) prepared by photo-polymerization in a capillary.

broad peak based upon the lateral diffraction of mesogenic group for DM2 was observed in the wide-angle region of the X-ray diffraction pattern. These results of X-ray measurements and microscopic observation support that DM2 exhibited a nematic phase.

Epoxy resin 1 (ER1) was prepared by photo-polymerization of DM1 at 140°C. A schlieren texture is also observed for ER1 at room temperature. This result indicates that the nematic structure of DM1 is fixed by photo-polymerization. To make sure of the phase structure of ERl, X-ray diffraction measurements were carried out for ER1 prepared by photo-polymerization in quartz capillary (diameter 1 mm). Figure 3a supports that ER1 demonstrates a nematic structure. However, the mesogenic groups in ER1 would be closely packed compared to those in conventional nematic structures, because the peak in the wide angle is slightly sharp.

ER2 was also prepared by photo-polymerization of DM2 at 120°C (smectic phase). The homeotropic alignment of mesogenic group in ER2 was fixed at room temperature after photo-polymerization.

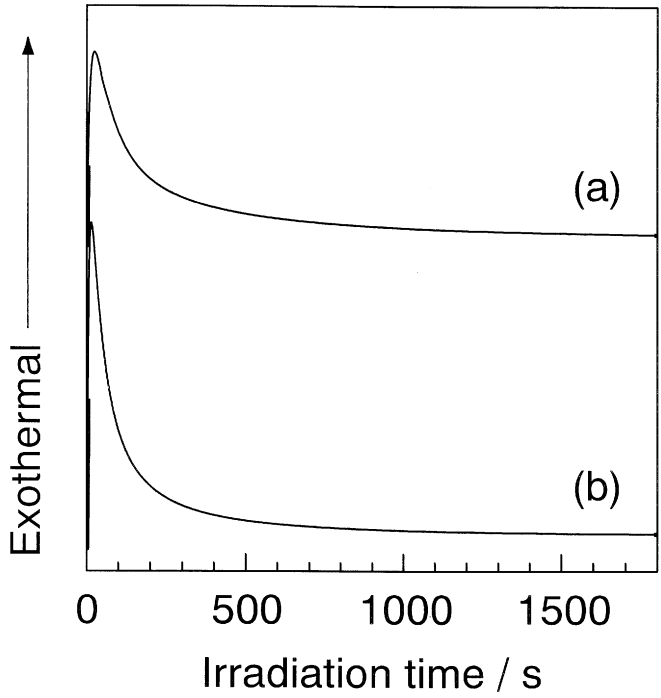

FIGURE 4 Isothermal DSC curves for the photo-polymerization of diepoxy monomer 1 at 140°C (a) and of diepoxy monomer 2 at 120°C (b).

Figure 3b shows the X-ray diffraction pattern of ER2 prepared by photo-polymerization in capillary. The X-ray diffraction pattern supports that ER2 had a smectic structure. The layer spacing of the smectic structure for ER2 was 48 Å based upon the sharp peak in the small-angle region. The layer spacing of the smectic structure for ER2 was similar to that for DM2. This result indicates that the smectic structure similar to that of DM2 is fixed in ER2 by photo-polymerization.

The reaction time for photo-polymerization of DMs was investigated by isothermal UV-DSC measurements. Figure 4 shows the isothermal DSC curves for the photo-polymerization of DMs. The photo-polymerization rate of DMs increased rapidly after ultraviolet (UV) irradiation for 2–3 s and a maximum of photo-polymerization rate was reached after UV irradiation for 15–25 s. Then, the photo-polymerization rate decreased gradually. The decrease in photo-polymerization rate may be explained by the increase in viscosity of the epoxy resin, depletion of the monomer, and decrease in diffusion of the monomer during

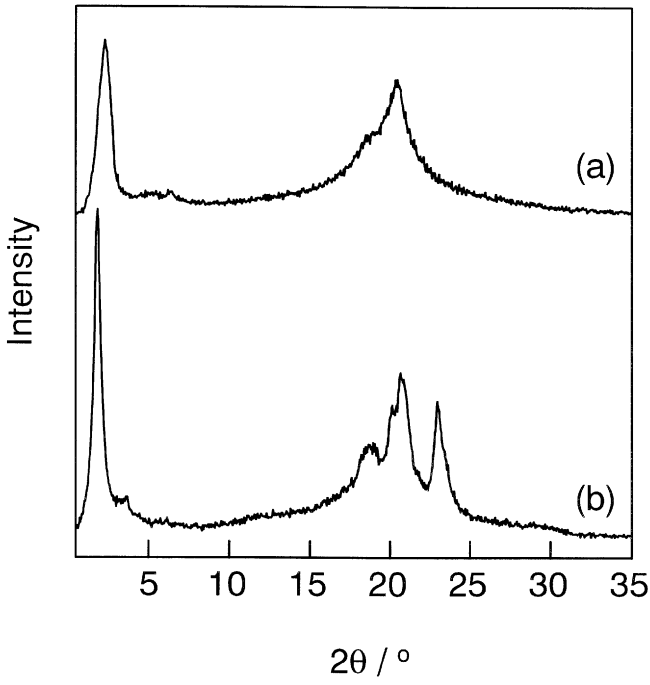

FIGURE 5 X-ray patterns of thick films of epoxy resins 1 (a) and 2 (b).

photo-polymerization. The DSC curves indicated that equilibrium state of photo-polymerization was reached after UV irradiation for about 10 min.

The extent of photo-polymerization was confirmed based upon the absorbance ratio of the peaks near 912 cm^{-1} and 1733 cm^{-1} by Fourier transform infrared (FT-IR) measurements. The peaks near 912 cm^{-1} and 1733 cm^{-1} are attributed to C−C stretching vibration of epoxy ring and C=O stretching vibration of ester group, respectively. The extent of photo-polymerization for DM1 in the nematic phase and DM2 in the smectic phase is 61% and 76%, respectively. The extent of photo-polymerization of DM2 in the smectic phase is slightly larger than that of DM1 in the nematic phase. The structure of mesophase for DMs would play an important role in the extent of photo-polymerization. However, details of the effect of mesophase structure on the extent of photo-polymerization are not clarified at the present time.

We described the extent of photo-polymerization for DMs and the phase structure of ERs in the thin-film state (thickness: about 10 μm). We also prepared thick films of ERs (about 1 mm in thickness)

TABLE 2 Thermal Decomposition Temperatures of Epoxy Resins

Epoxy resins (photo-polymerization temperature)	T_d/°C[a]
ER1 (140°C, nematic)	289
ER2 (120°C, smectic)	311

[a]Temperatures at which 10% weight loss was recorded by TGA measurements.

and investigated the phase structure of the thick films. Figure 5 shows the X-ray diffraction patterns of ER films about 1 mm in thickness. The X-ray diffraction pattern of thick films of ER1 displays that ER1 would have a smectic-like structure based upon the sharp peak near 2.3° (d-spacing; 38 Å). However, ER1 also has a crystalline-like structure, because the peak near 20°, attributed to lateral spacing between mesogenic groups, is very sharp. ER1 in the thin-film state possesses a nematic structure; however, ER1 in the thick-film state would have both smectic and crystalline structures. ER2 in the thick-film state would have a crystalline-like structure rather than a smectic-like structure as shown in Fig. 5b. These results indicate that the phase structure of ERs would depend upon the film thickness for photo-polymerization; however, we cannot clarify the reason why the phase structure of ERs depends upon the film thickness for photo-polymerization at the present time.

Thermal-degradation temperatures (T_d) are recorded at the temperature at which 10% weight loss of the thick films of ERs occurred. T_ds of ERs are summarized in Table 2. ERs are thermally stable until about 290°C. T_d of ER2 is higher than that of ER1. FT-IR measurements reveal that the extent of photo-polymerization for DM2 in the smectic phase is slightly larger than that for DM1 in the nematic

TABLE 3 Thermal Conductivity of Epoxy Resins

Epoxy resins (photo-polymerization temperature)	Density (ρ)/($g\,cm^{-3}$)	Heat capacity (C_p)/($J\,g^{-1}\,K^{-1}$)	Thermal diffusivity (α)/($10^{-3}\,cm^2\,s^{-1}$)	Thermal conductivity (λ at 25°C/)/($W\,m^{-1}\,K^{-1}$)[a]
ER1 (140°C, nematic)	1.16	1.50	1.76	0.31
ER2 (120°C, smectic)	1.12	1.41	2.71	0.43

[a]$\lambda = \rho\, C_p\, \alpha$.

phase, although the sample thickness for the photo-polymerization of DMs is thin (10 μm in thickness) compared to that for TGA measurements. Therefore, T_d of ERs would correlate with the extent of photo-polymerization.

Thermal conductivity of ERs in the thick-film state is summarized in Table 3. Thermal conductivity of ER2 prepared by photo-polymerization in the smectic phase is larger than that of ER1 photo-polymerized in the nematic phase. The higher orientational order of mesogenic groups in the resulting ER2 and larger conversion of DM2 are obtained by photo-polymerization of DM2 in the smectic phase. Therefore, thermal conductivity of ERs would be deeply dependent upon the conversion of DMs and the orientational order of mesogenic groups in the resulting ERs. Details of the relationship between thermal conductivity of the resulting ERs and the polymerization condition of LC diepoxy monomers would be clarified by further investigation.

The values of thermal conductivity ($0.43\,W\,m-1K-1$) and 0.31 $W\,m^{-1}\,K^{-1}$ of ERs are larger than that of conventional epoxy resins (about $0.2\,W\,m-1K-1$). This result demonstrated that highly ordered phase structure was favorable for suppressing phonon scattering.

REFERENCES

[1] Hilmet, R. A. H. & Kemperman, H. (1998). *Nature*, *392*, 476–479.
[2] Broer, D. J., Mol, G. N., van Haaren, J. A. M. M., & Lub, J. (1999). *Adv. Mater.*, *11*, 573–578.
[3] Terentjev, E. M. (1999). *J. Phys.: Condens. Matter*, *11*, R239–R257.
[4] Broer, D. J., Hikmet, R. A. M., & Challa, G. (1989). *Makromol. Chem.*, *190*, 3201–3215.
[5] Broer, D. J., Boven, J., Mol, G. N., & Challa, G. (1989). *Makromol. Chem.*, *190*, 2255–2268.
[6] Broer, D. J., Mol, G. N., & Challa, G. (1991). *Makromol. Chem.*, *192*, 59–74.
[7] Shiota, A. & Ober, C. K. (1996). *J. Polym., Part A: Polym. Sci. Chem.*, *34*, 1291–1303.
[8] Mallon, J. J. & Adams, P. M. (1993). *J. Polym. Sci. Part A: Polym. Chem.*, *31*, 2249–2260.
[9] Carfagna, C., Amendola, E., & Giamberini, M. (1994). *Macromol. Chem. Phys.*, *195*, 279–287.
[10] Jahromi, S. & Mijs, W. J. (1994). *Mol. Cryst. Liq. Cryst.*, *250*, 209–222.
[11] Giamberini, M., Amendola, E., & Carfagna, C. (1995). *Mol. Cryst. Liq. Cryst. Sci. Technol.*, Section A, *266*, 9–22.
[12] Mormann, W. & Bröcher, M. (1996). *Macromol. Chem. Phys.*, *197*, 1841–1851.
[13] Grebowicz, J. S. (1996). *Macromol, Symp.*, *104*, 191–221.
[14] Farren, C., Akatsuka, M., Takezawa, Y., & Itoh, Y. (2001). *Polymer*, *42*, 1507–1514.
[15] Takezawa, Y. (2002). *Purasuchikkusu Eji*, *48*, 134–137.
[16] Akatsuka, M. & Takezawa, Y. (2003). *J. Appl. Polym. Sci.*, *89*, 2464–2467.
[17] Jahromi, S., Lub, J., & Mol, G. N. (1994). *Polymer*, *35*, 622–629.
[18] Broer, D. J., Lub, J., & Mol, G. N. (1993). *Macromolecules*, *26*, 1244–1247.